

# **A BENEFIT ASSESSMENT OF USING IN-CORE NEUTRON DETECTOR SIGNALS IN CORE PROTECTION CALCULATOR SYSTEM (CPCS)**

**Seung Han, Suk-Joon Park**

Korea Atomic Energy Research Institute

**Poong-Hyun Seong**

Korea Advanced Institute of Science and Technology

## **Abstract**

A Core Protection Calculator System (CPCS) is a digital computer based safety system generating trip signals based on the calculation of Departure from Nucleate Boiling Ratio (DNBR) and Local Power Density (LPD). Currently, CPCS uses ex-core detector signals for core power calculation and it has some uncertainties.

In this study, in-core detector signals which directly measure inside flux of core are applied to CPCS to get more accurate power distribution profile, DNBR and LPD. In order to improve axial power distribution calculation, piece-wise cubic spline method is applied; from the 40 nodes of expanded signals, more accurate and detailed core information can be provided. Simulation is carried out to verify its applicability to power distribution calculation. Simulation result shows that the improved method reduces the calculational uncertainties significantly and it allows larger operational margin. It is also expected that no power reduction is required while Core Operating Limit Supervisory System (COLSS) is out-of-service due to reduced uncertainties when the improved method is applied. In this study, a quantitative economic benefit assessment of using in-core neutron detector signals is also carried out.

## **Introduction**

In Yonggwang Nuclear Power Plant Units 3 and 4 (YGN Units 3,4), the Core Protection Calculator System (CPCS) which is a digital computer based safety system generates low Departure from Nucleate Boiling Ratio (DNBR) and high Local Power Density (LPD) trip signals based on the incoming process variables [1]. Currently, CPCS uses ex-core detector signals for core power calculation. For sensor utilisation aspect, ex-core neutron detectors which provide signals for power calculation in current CPCS can generate electric signal fast enough for calculations in CPCS but the conversion of the ex-core detector signals to internal core power is less accurate than direct measurement. What is worse, this inaccuracy for power calculations from indirect measuring method affect plant operation also. In this study, in-core detector signals which directly measure inside flux of core are applied to CPCS to get more accurate power distribution profile, DNBR and LPD. Two hundred twenty-five numbers of in-core neutron detector signals in total can be acquired to get core power information. Applying these in-core signals to CPCS, power distribution calculation can be more accurate than in current CPCS because of the direct measurement of core power and the reduction of calculation uncertainties. This improvement for power distribution calculation can cause some benefits, such as increasing thermal margin, assuring operational flexibility during normal operation and economical cost reduction due to no reduction of power while Core Operating Limit Supervisory System (COLSS) [2] is out-of service.

## **CPC power calculation algorithm**

### ***Power distribution algorithm***

The purpose of the power distribution calculation is to compute the core average axial power distribution, pseudo hot pin power distribution, and the three dimensional power peak from the ex-core detector signals and the target CEA positions. The ex-core detector signals, CEA positions, and the temperature shadowing factor are also used to compute a power normalisation factor required for calculation of calibrated neutron flux power.

After analogue to digital converting and range checking for input processing, engineering values from each of three axial segments of a single ex-core detector stack are received. Several compensation methodologies are applied then for their concurrence with power inside of core such as shape annealing which is converting ex-core signals to peripheral power fractions at each axial level, CEA shadowing factor applying which is converting peripheral power fractions to core average power fractions at each axial level depending on CEA configuration. Axial power shape is calculated based on the values calculated from compensations.

## **Core power calculation with in-core detector signal**

Improved power distribution calculation method uses in-core neutron detector signals instead of ex-core neutron detector signal for calculation inputs. The method implemented in this study provides the following:

- Calculation of axial power distribution including in-core detector signals;
- Calculation of axial shape index;
- Predict the highest LPD based on in-core power signals;
- Predict the lowest DNBR based on in-core power signals.

### ***In-core signal input processing***

Dynamic compensation of the in-core neutron detector signals is performed to compensate the corrected detector signal for the beta decay behaviour of the rhodium detector element as follows:

Inputs:

S(I,J): In-core neutron detector signal, I = 1 to 45, J = 1 to 5

CS(I,J): Compensated rhodium detector signal

Output:  $CSI,J(KT) = J1*CS I,J(KT-T) + J3*S I,J(KT) + J4*S I,J(KT-T)$

### ***Conversion of in-core flux to power***

This routine converts in-core detector compensated neutron flux to assembly power at each in-core detector location. CEA configuration dependent correction factors are calculated for use in converting the compensated in-core detector flux CS(I,J) to power PHI(I,J). The calculation of this conversion factor is performed in two steps:

- Calculation of the fractional insertion of each CEA group in each of the five detector axial levels;
- Conversion of the insertion fraction to a correction for detector string I at level J.

### ***Calculation of fractional insertion***

For all CEA groups, the group fractional insertion is calculated by examining the lower and the lowest CEA. The fractional insertion is determined by calculating the distance between the lower tip of the CEA and the top of the axial detector level. The ratio of this distance to the level height is limited to be between 1.0 representing full insertion and 0.0 representing no insertion giving the fractional insertion. To make calculation of correction factors more convenient, the fractional insertions are stored in a look-up table matrix.

### Calculation of CEA correction factors

The CEA correction factor matrix is calculated from the CEA group fractional insertion matrix by matrix multiplication.

$$WRD(I,J) = \sum_{K=1}^{12} (C(I,K) * RP(K,J))$$

The CEA insertion correction, the burnup correction and a power dependent correction are applied to calculate the assembly power matrix PHI(I,J) for detector string I at level J. The power correction factor is used to adjust the burnup dependent correction WP(I,J) to give the unrodded conversion factor W(I,J) used to convert the flux in string I at level J to power.

$$W(I,J) = K(I) * WP(I,J)$$

The power for string I at level J is computed as:

$$PHI(I,J) = CS(I,J) * (W(I,J) + WRD(I,J))$$

### Axial power distribution

The cubic spline synthesis [3,4] is to assume the axial power to be a sum of splines in which each spline is a piece-wise cubic expression. The breakpoints between splines are chosen based on relative in-core detector signals.

Modelling:

$$\Phi(Z) = \sum_{j=1}^9 A_j \mu_j(z) \quad (1)$$

The cubic spline basic function is defined as follows:

$$\begin{aligned} \mu_j(z) &= f_1(\eta_1) & Z_{i-2} \leq Z \leq Z_{i-1} & \quad \mu_j(z) = f_2(\eta_2) & \quad Z_{i-1} \leq Z \leq Z_i \\ \mu_j(z) &= f_2(\eta_3) & Z_i \leq Z \leq Z_{i+1} & \quad \mu_j(z) = f_1(\eta_4) & \quad Z_{i+1} \leq Z \leq Z_{i+2} \\ \mu_j(z) &= 0 & Z > Z_{i+2} \text{ or } Z < Z_{i-2} & \end{aligned}$$

Where:

$$\begin{aligned} \eta_1 &= (Z - Z_{i-2}) / (Z_{i-1} - Z_{i-2}), & \eta_2 &= (Z - Z_{i-1}) / (Z_i - Z_{i-1}) \\ \eta_3 &= (Z_{i+1} - Z) / (Z_{i+1} - Z_i), & \eta_4 &= (Z_{i+2} - Z) / (Z_{i+2} - Z_{i+1}) \end{aligned}$$

$$f_1(\eta) = \eta^3 / 4, \quad f_2(\eta) = 1/4 + 3(\eta + \eta^2 - \eta^3) / 4 \quad (2)$$

The various axial power shapes are categorised depending on the characteristics, i.e. centre peak, saddle type or flat. Appropriate number of nodes for each interval is assigned based on the categorised power shapes. It should be noted that the total number of axial nodes for each node set is same. The amplitude coefficients are found to satisfy the following conditions:

- Detector responses

$$D_i = \int_i \Phi(z) dz \quad (3)$$

- Two empirical boundary conditions

$$\Phi(0) = \alpha_1 * D_5 + \alpha_2 \text{ (top)}, \Phi(H) = \alpha_3 * D_1 + \alpha_4 \text{ (bottom)} \quad (4)$$

- Two extrapolated boundary conditions

$$\Phi(-\delta) = 0.0, \Phi(H + \delta) = 0.0 \quad (5)$$

Using equation (1), equations (3), (4) and (5) can be expressed as follows :

$$\begin{aligned} B_1 &= H_{11}A_1 + H_{12}A_2 + \dots + H_{19}A_9 \\ &\vdots \\ &\vdots \\ B_9 &= H_{91}A_1 + H_{92}A_2 + \dots + H_{99}A_9 \end{aligned} \quad (6)$$

Equation (6) is rewritten in a matrix form of amplitude coefficients:

$$\bar{A} = \bar{H}^{-1} * \bar{B}$$

The axial power FZI(I,J) for those nodes J in assembly I is obtained as follows:

$$FZI(i,j) = A(j) * TERM(i)$$

### ***Axial shape index***

The power in upper and lower halves of the core are calculated from the 40 node axial power distribution.

$$SUML = \sum_{I=1}^{45} \sum_{J=1}^{20} FZI(I, J)$$

$$SUMU = \sum_{I=1}^{45} \sum_{J=21}^{40} FZI(I, J)$$

For axial shape index calculation,

$$ASI = \frac{SUML - SUMU}{SUML + SUMU}$$

## **Simulation results and discussion**

### ***Simulation***

In order to prove and demonstrate the applicability of improved power distribution calculation method using in-core neutron detector signals to CPCS, various simulations were carried out. The CPC FORTRAN simulation code [5] was used for simulation of improved method with actual plant data. And the Reactor Operation and Control Simulator (ROCS) code [6] was used to generate the data for various plant mode such as Begin Of Cycle (BOC), Middle Of Cycle (MOC) and End Of Cycle (EOC) to compare with the axial power distribution profile from improved method.

#### *Actual plant data simulation*

Since improved power distribution calculation method is implemented on CPC FORTRAN, actual plant data from Yonggwang Nuclear Power Plant Unit 3 were used to verify the integrity of the new method. Data were acquired at 100 % steady state power. Input arrays for in-core neutron detector signals were generated to execute the CPC FORTRAN. Simulation results are shown in Table 1. Also, Figure 1 shows the core power distribution profile with side view.

#### *Various plant mode simulation*

In order to prove the accuracy of piece-wise cubic spline method for power distribution using in-core neutron detector signals, various plant states along with burnup rate were chosen. ROCS provides axial power distribution for each burnup rate and pseudo in-core detector signals, respectively at 3030 MWD/T (BOC), 7005 MWD/T (MOC) and 11300 MWD/T.

### ***Discussion***

#### *Uncertainty comparison*

As shown in Table 1, results of simulation with actual plant data of in-core detector signals show more stringent values than those of current CPCS. As mentioned earlier, in-core neutron detectors are located inside the core and measure core power directly and one can expect this result. It is important however to review the latent uncertainties between improved algorithm with in-core neutron detector signals and current algorithm with ex-core ones, because calculational uncertainties can affect the thermal margin. Comparison was carried out by estimating sensor uncertainties, calculation uncertainties to get total values. Following are the uncertainty estimations for both cases:

- Current algorithm with ex-core detector signals

Total Channel Error : +/- 1.27 % FS

Since Full Scale (FS) range for the Ex-core channel is 200 % power, error conversion to percent power is:

$$\pm 1.27 \times 200 = \pm 2.54 \% P$$

Results of uncertainty calculation are:

Uncertainty for neutron flux power used in DNBR: 2.5% P

Uncertainty for power used in LPD: 12% P

Hot pin ASI uncertainty: 0.0715

- Improved algorithm with in-core detector signals

Total Channel Error : +/- 0.2778 % FS

Since Full Scale (FS) range for the in-core channel is 333 % power, error conversion to percent power is:

$$\pm 0.2778 * 333 = \pm 0.925074 \% P$$

Results of uncertainty calculation are:

Uncertainty for neutron flux power used in DNBR: 0.05 % P

Uncertainty for power used in LPD: 1.12 % P

Hot pin ASI uncertainty: -0.02297, 0.01554

According to the above comparison, improved method offers significant reduction in uncertainties. Figure 2 shows the comparison of thermal margin and operational flexibility with uncertainty when using current algorithm and improved algorithm.

#### *Axial shape error calculation*

The core axial power shapes and in-core signals for various operating conditions were generated by using a best estimate neutronics computer code, ROCS. The error for power distribution between the ROCS and improved algorithm axial power shape is defined as:

$$E_i^k = \left[ \frac{Fz(i)_{CPC} - Fz(i)_{ROCS}}{Fz(i)_{ROCS}} \right] * 100.0$$

The root-mean-square error (RMS) is then calculated by:

$$RMS^k = \sqrt{\frac{\sum_{i=1}^{20} (E_i^k)^2}{20}}$$

RMS errors from current axial power distribution method, fourier series 5 weighting synthesis in COLSS, show 10.4 %, 16% and 5.8% respectively at 3030 MWD/T, 7005 MWD/T and 11300 MWD/T. RMS error values for the three representative axial shapes are decreased to 5.4%, 10.5% and 3.9% respectively by applying the improved algorithm.

With these simulation results, we expect that no power reduction is required while COLSS is out of service, which is currently one of the technical specification requirements. In other words, current nuclear power plant which uses CPCS and COLSS must derate the power to 85% for its operating limit with poor uncertainties in CPCS when COLSS is

out-of-service, but no power reduction is required even if COLSS is out of service by applying the improved algorithm which is using in-core neutron detector signals for power distribution calculation.

### *Benefit assessment*

We can consider the benefit of applying the improved power distribution algorithm to Core Protection Calculator System in two kinds of viewpoints. One is the operational benefit viewpoint and the other is the economical benefit viewpoint.

From the operational viewpoint, reduction in uncertainties brings higher operational flexibility possibly which can reduce the number of unscheduled reactor shutdown. Large uncertainties in CPCS for power calculation using ex-core detector signals require reduction of power to 85% while COLSS is out-of-service. Therefore, when we get more accurate power distribution using in-core neutron detector signals in CPCS, we can operate power plant at 100% power without any power reduction even when COLSS is out-of-service.

From the economical viewpoint, capacity factor is one of the major measures of economic assessment [7,8,9], which is to measure the total electrical power produced in some period of time for operating power plant. Capacity factor is defined as follows:

*Capacity factor:* Percent of the total electrical power which could theoretically be produced during a specified period if plant were operated at full power one hundred percent of time:

$$\left[ \sum_i (\text{Operating days} * \text{Electrical power in that period}) \right] / (\text{Electrically full power} * \text{Total days in one period})$$

The capacity factor of the power plant with current CPCS can be modelled as follows:

$$C1 = [1 * (365 - \text{MTTR}_{\text{COLSS}} - \text{USRSP1} - \text{SRSP}) + 0.85 * \text{MTTR}_{\text{COLSS}} + 0 * (\text{USRSP1} + \text{SRSP})] / 365$$

For the power plant with the CPCS of improved algorithm,

$$C2 = [1 * (365 - \text{USRSP2} - \text{SRSP}) + 0 * (\text{USRSP2} + \text{SRSP})] / 365$$

If we can operate power plant with CPCS of improved power distribution algorithm when COLSS is out-of-service, C2 will be larger than C1 because there is no need of power reduction from 100% power to 85% power. This means COLSS MTTR does not affect power reduction any more. Higher capacity factor consequently reduces electricity generation cost. Increasing thermal margin and operational flexibility, we can also expect that the number of unscheduled reactor shutdown will be reduced ( $\text{USRSP1} > \text{USRSP2}$ ) and it results in capacity factor increasing.

In qualitative terms, capacity factor will be increased when using in-core detector signals in Core Protection Calculator System and increasing in capacity factor will result in electricity generation cost savings for the whole plant life time.



### *Sensitivity analysis*

Since YGN Unit 3 started its operation in 1994, we cannot get the data of Mean Time To Repair (MTTR) for COLSS. Economic benefit assessment in terms of electricity generation cost with improved algorithm was carried out by sensitivity analysis. The various values of COLSS MTTR and Mean Time To Failure (MTTF) were applied to identify the effect of capacity factor on cost.

Followings are the inputs for the analysis:

- Scheduled Reactor Shutdown Period [10]: 60 days
- Unscheduled Reactor Shutdown Period [10]: 5 days
- One Cycle Period: 365 days
- Power Output Rating: 1050 MWe
- Plant Life Time: 30 years
- COLSS MTTR changes: 1 day, 2 days, 5 days, 10 days, 20 days, 30 days
- COLSS MTTF changes: 1 yr., 2 yrs., 5 yrs., 10 yrs., 20 yrs.

With these data, capacity factors were calculated for each MTTR and electricity generation cost were calculated by executing the electricity generation cost program [11]. Table 2 shows the capacity factors and cost changes at various COLSS MTTRs. Figure 3 shows the total electricity generation cost for various COLSS MTTFs and MTTRs when applying improved algorithm to current CPCS. In Figure 4, we can easily see the relationship between the life time benefit in economic terms and COLSS MTTRs and MTTFs.

### **Conclusion and further study**

The current Core Protection Calculator System (CPCS) calculates core power using ex-core neutron detector signals and it has considerable amount of uncertainties due to indirect measurement. In order to improve the power distribution calculation, we have applied in-core neutron detector signals which measure inside flux of core directly to CPCS in this study. The piecewise cubic spline synthesis was used for more detailed power distribution calculation.

In order to demonstrate its applicability to Core Protection Calculation algorithm, two simulations were carried out. One was simulation using actual plant data of in-core detector signals which were from Yonggwang Unit 3 100% power steady state, and the other was one using various plant burnup data from best estimate reactor simulation code, ROCS. We also compared the simulated results from improved method with those from current CPC method. From the results of the first simulation, we have found that improved method provided more accurate power distribution profile and more detailed core information and assured increasing of thermal margin and operational flexibility due to

the reduction of uncertainties. From the second simulation, we have evaluated that power distribution calculation of improved algorithm provided more accurate profile at various plant burnup state than current power distribution calculation.

Then we performed a benefit assessment of using in-core signals in actual CPCS and suggested that there was no need of power reduction to 85% while COLSS was out-of-service. It was also identified that the assurance of improved operation flexibility resulted in reduction of the electricity generation cost for plant life time.

However, before we apply this method to actual plant Core Protection Calculator System, each in-core neutron detector channel identification is needed because CPCS has four channels and in-core signal input processing cards are needed for each channel. And also the study on in-core sensor life expansion is needed to apply this method to safety system, CPCS, because current in-core neutron detectors are not qualified as safety equipments.

## NOMENCLATURE

I	No. of in-core detector assembly
J	No. of in-core detector level in axial position
$CS_{i,j}(KT)$	Compensated signal of detector (I,J) at time (KT)
$CS_{i,j}(KT-T)$	Compensated signal of detector (I,J) at time (KT-T)
$S_{i,j}(KT)$	Uncompensated signal of detector (I,J) at time (KT)
$S_{i,j}(KT-T)$	Uncompensated signal of detector (I,J) at time (KT-T)
J1, J3, J4	Constants
$WRD(I,J)$	CEA correction factor
$C(I,K)$	Matrix, shadowing of string I by CEA group K
$RP(K,J)$	Insertion of CEA group K in level J
$W(I,J)$	Unrodded correction factor for string I level J
$WP(I,J)$	Burnup dependent correction factor for string I level J
$K(I)$	Correlation constants for string I
$PHI(I,J)$	Assembly power in string I level J
$CS(I,J)$	Compensated detector flux for string I
$\Phi(Z)$	Power at core altitude Z
$A_j$	Amplitude coefficient
$\mu_j(z)$	Value of jth spline function at z
$D_i$	Detector responses
$\alpha_1 \alpha_2 \alpha_3 \alpha_4$	Boundary point coefficients
$\delta$	Extrapolated length
H	Core height
$\bar{A}$	Vector of spline amplitudes
$\bar{H}^{-1}$	Pre-calculated spline matrix
$\bar{B}$	Vector of detector responses and boundary point
$FZI(i,j)$	Related axial power at node j in assembly i
TERM(i)	Array of pre-calculated values for spline function
SUML	Relative power in the lower half of the core
SUMU	Relative power in the upper half of the core
$FZI(I,J)$	Related axial power at node J in assembly I
$Fz(i)$	Normalised axial power at node I
K	Case counter
C1, C2	Capacity Factor
$MTTR_{COLSS}$	COLSS Mean Time To Repair
USRSP1,2	Unscheduled Reactor Shutdown Period
SRSP	Scheduled Reactor Shutdown Period

## REFERENCES

- [1] Combustion Engineering Inc., "Functional Design Requirements for a Core Protection Calculator," CEN-305-P, Revision 02-P, 1988.
- [2] Combustion Engineering Inc., "Functional Design Requirements for a Core Operating Limit Supervisory System (COLSS) for Yonggwang Nuclear Units 3 and 4," CE-NPSD-423-P, Rev. 1-P, 1988.
- [3] S.D. Conte, Carl de Boor, "Engineering Numerical Analysis," 3rd Edition, McGraw-Hill Inc., 1981.
- [4] R.L. Burden, A.C. Reynolds, "Numerical Analysis," 2nd Edition, PWS Publishers, 1981.
- [5] User's Manual for the CPC/CEAC FORTRAN Simulation Code.
- [6] Combustion Engineering Inc., "User's Manual for ROCS," CE-CES-4-Rev. 3-P.
- [7] J.R. Lamarsh, "Introduction to Nuclear Engineering," 2nd Edition, Addison-Wesley Publishing Company, 1983.
- [8] G. Basso, W. Fusari, "In Search of Ageing Factors," International Conference on Nuclear Power Plant Ageing, Availability Factor and Reliability Analysis, 1985.
- [9] T.R. Wilson, G.C. Gower, "Evaluation of Nuclear Power Plant Availability," 1974, US Atomic Energy Commission.
- [10] Analysis of Outage Reports of Nuclear Power Plants in Korea, KAERI/TR-444/94.
- [11] Economic Analysis of Nuclear Power Generation, KAERI/RR-947-90.

**Table 1. Comparison of simulation results**

	ASI	LPD(Kw/ft)	DNBR
Current Algorithm	0.0707	13.2344	1.4773
New Algorithm	0.094	14.1657	1.4351

**Table 2. Capacity factor and cost changes at various COLSS MTTRs**

	<i>MTTR (day)</i>	<b>1</b>	<b>2</b>	<b>5</b>	<b>10</b>	<b>20</b>	<b>30</b>
<b>CURRENT</b>	Capacity Factor	0.8215	0.821	0.8198	0.8178	0.8136	0.809
<b>CPCS</b>	COST (Won/Kwh)	26.79	26.80	26.84	26.89	27.01	27.14
<b>IMPROVED</b>	Capacity Factor	0.8219	0.8219	0.8219	0.8219	0.8219	0.8219
<b>CPCS</b>	COST (Won/Kwh)	26.78	26.78	26.78	26.78	26.78	26.78

**Figure 1. Core power distribution profile**

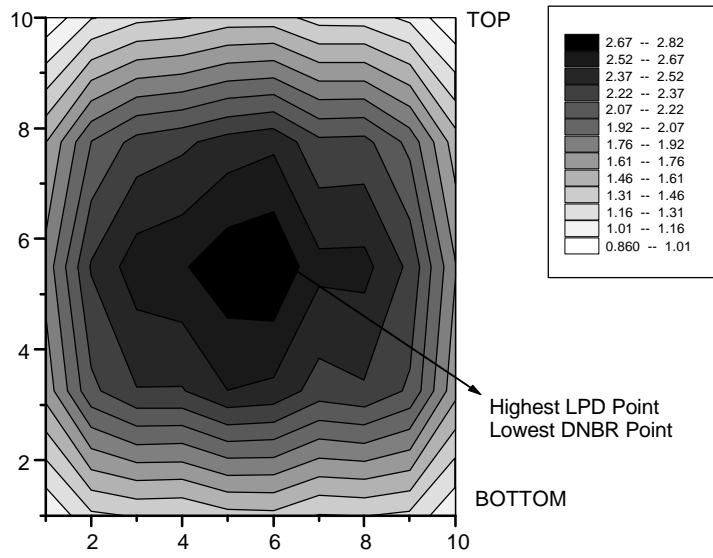


**Figure 2. Thermal margin and operational flexibility comparison**

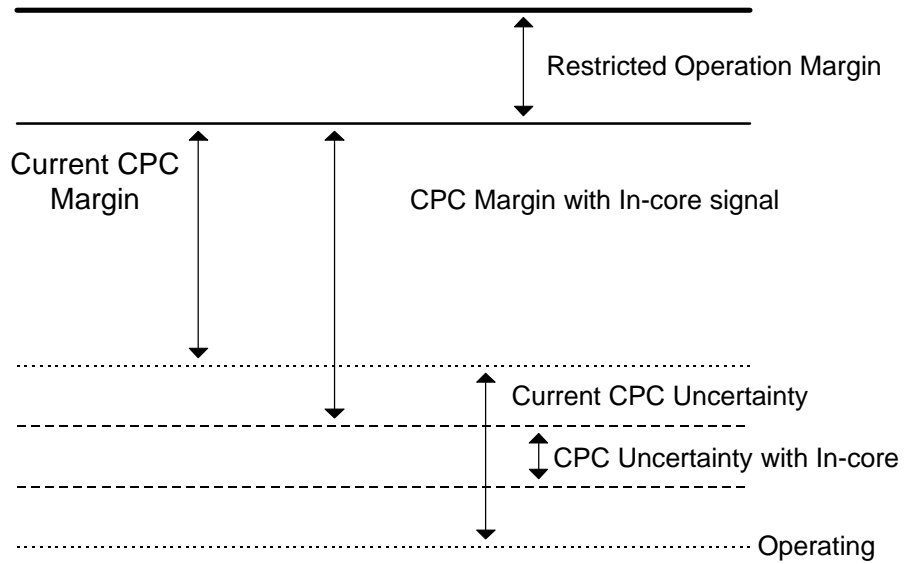


**Figure 3. Total electricity generation cost during plant life at various COLSS MTTRs**

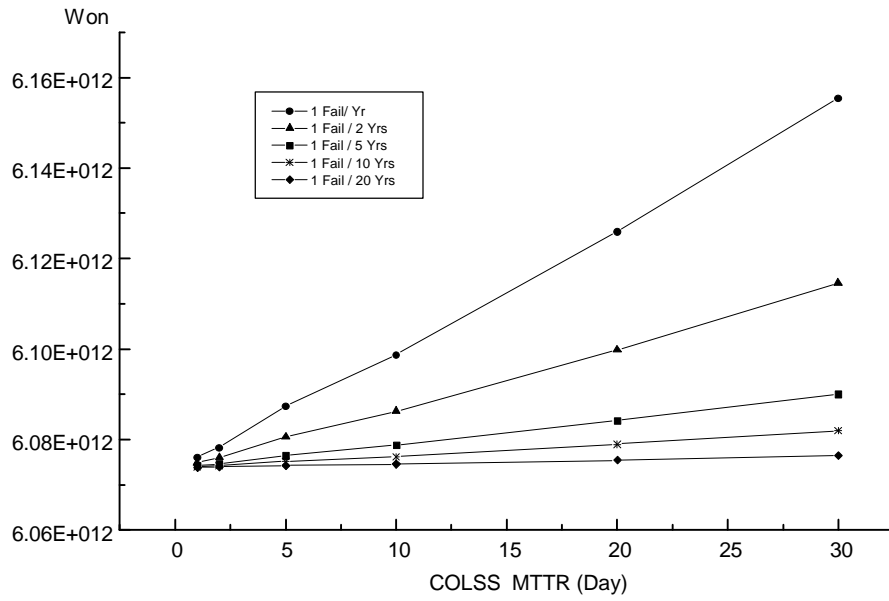


**Figure 4. Cost differences from capacity factor changes**

